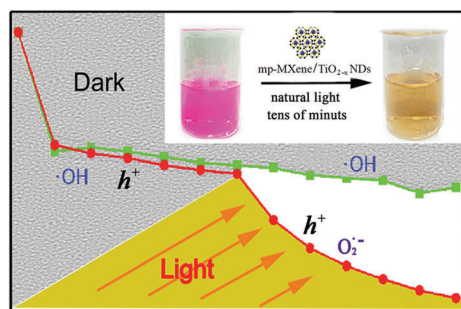


We have presented the Graphical Abstract text and image for your article below. This brief summary of your work will appear in the contents pages of the issue in which your article appears.



A titanium-based photo-Fenton bifunctional catalyst of mp-MXene/TiO_{2-x} nanodots for dramatic enhancement of catalytic efficiency in advanced oxidation processes

Xiaomei Cheng, Lianhai Zu, Yue Jiang, Donglu Shi, Xiaoming Cai, Yonghong Ni,* Sijie Lin* and Yao Qin*

A pseudo-Fenton reaction works synergistically with photocatalysis to greatly accelerate the oxidative degradation rate.

Please check this proof carefully. Our staff will not read it in detail after you have returned it.

Please send your corrections either as a copy of the proof PDF with electronic notes attached or as a list of corrections. **Do not edit the text within the PDF or send a revised manuscript** as we will not be able to apply your corrections. Corrections at this stage should be minor and not involve extensive changes.

Proof corrections must be returned as a single set of corrections, approved by all co-authors. No further corrections can be made after you have submitted your proof corrections as we will publish your article online as soon as possible after they are received.

Please ensure that:

- The spelling and format of all author names and affiliations are checked carefully. You can check how we have identified the authors' first and last names in the researcher information table on the next page. **Names will be indexed and cited as shown on the proof, so these must be correct.**
- Any funding bodies have been acknowledged appropriately and included both in the paper and in the funder information table on the next page.
- All of the editor's queries are answered.
- Any necessary attachments, such as updated images or ESI files, are provided.

Translation errors can occur during conversion to typesetting systems so you need to read the whole proof. In particular please check tables, equations, numerical data, figures and graphics, and references carefully.

Please return your **final** corrections, where possible within **48 hours** of receipt, by e-mail to: chemcomm@rsc.org. If you require more time, please notify us by email.

Funding information

Providing accurate funding information will enable us to help you comply with your funders' reporting mandates. Clear acknowledgement of funder support is an important consideration in funding evaluation and can increase your chances of securing funding in the future.

We work closely with Crossref to make your research discoverable through the Funding Data search tool (<http://search.crossref.org/funding>). Funding Data provides a reliable way to track the impact of the work that funders support. Accurate funder information will also help us (i) identify articles that are mandated to be deposited in **PubMed Central (PMC)** and deposit these on your behalf, and (ii) identify articles funded as part of the **CHORUS** initiative and display the Accepted Manuscript on our web site after an embargo period of 12 months.

Further information can be found on our webpage (<http://rsc.li/funding-info>).

What we do with funding information

We have combined the information you gave us on submission with the information in your acknowledgements. This will help ensure the funding information is as complete as possible and matches funders listed in the Crossref Funder Registry.

If a funding organisation you included in your acknowledgements or on submission of your article is not currently listed in the registry it will not appear in the table on this page. We can only deposit data if funders are already listed in the Crossref Funder Registry, but we will pass all funding information on to Crossref so that additional funders can be included in future.

Please check your funding information

The table below contains the information we will share with Crossref so that your article can be found *via* the Funding Data search tool. **Please check that the funder names and grant numbers in the table are correct and indicate if any changes are necessary to the Acknowledgements text.**

Funder name	Funder's main country of origin	Funder ID (for RSC use only)	Award/grant number
National Natural Science Foundation of China	China	501100001809	21607115, 21777116, 21571005

Q1

Researcher information

Please check that the researcher information in the table below is correct, including the spelling and formatting of all author names, and that the authors' first, middle and last names have been correctly identified. **Names will be indexed and cited as shown on the proof, so these must be correct.**

If any authors have ORCID or ResearcherID details that are not listed below, please provide these with your proof corrections. Please ensure that the ORCID and ResearcherID details listed below have been assigned to the correct author. Authors should have their own unique ORCID iD and should not use another researcher's, as errors will delay publication.

Please also update your account on our online [manuscript submission system](#) to add your ORCID details, which will then be automatically included in all future submissions. See [here](#) for step-by-step instructions and more information on author identifiers.

First (given) and middle name(s)	Last (family) name(s)	ResearcherID	ORCID iD
Xiaomei	Cheng		
Lianhai	Zu	N-5979-2016	
Yue	Jiang		
Donglu	Shi		
Xiaoming	Cai		
Yonghong	Ni		0000-0002-4979-9867
Sijie	Lin		0000-0002-6970-8221
Yao	Qin		0000-0001-9880-7301

Queries for the attention of the authors

Journal: ChemComm

Paper: c8cc05866k

Title: **A titanium-based photo-Fenton bifunctional catalyst of mp-MXene/TiO_{2-x} nanodots for dramatic enhancement of catalytic efficiency in advanced oxidation processes**

For your information: You can cite this article before you receive notification of the page numbers by using the following format: (authors), Chem. Commun., (year), DOI: 10.1039/c8cc05866k.

Editor's queries are marked on your proof like this **Q1**, **Q2**, etc. and for your convenience line numbers are indicated like this 5, 10, 15, ...

Please ensure that all queries are answered when returning your proof corrections so that publication of your article is not delayed.

Query reference	Query	Remarks
Q1	Funder details have been incorporated in the funder table using information provided in the article text. Please check that the funder information in the table is correct.	
Q2	Please confirm that the spelling and format of all author names is correct. Names will be indexed and cited as shown on the proof, so these must be correct. No late corrections can be made.	
Q3	Do you wish to add an e-mail address for the corresponding author? If so, please provide the relevant information.	
Q4	"minutes" appears to be spelled incorrectly as "minuts" in the Graphical Abstract image. Please could you supply a corrected version (preferably as a TIF file at 600 dots per inch) with your proof corrections.	
Q5	The meaning of the sentence beginning "As Zhang <i>et al.</i> ..." is not clear – please provide alternative text.	
Q6	The sentence beginning "It is noteworthy..." has been altered for clarity. Please check that the meaning is correct.	
Q7	The sentence beginning "To investigate the..." has been altered for clarity. Please check that the meaning is correct.	
Q8	The sentence beginning "Interestingly, after light..." has been altered for clarity. Please check that the meaning is correct.	

10 **A titanium-based photo-Fenton bifunctional catalyst of mp-MXene/TiO_{2-x} nanodots for dramatic enhancement of catalytic efficiency in advanced oxidation processes†**

Cite this: DOI: 10.1039/c8cc05866k

Received 19th July 2018,
Accepted 17th September 2018

15 DOI: 10.1039/c8cc05866k

Xiaomei Cheng,^a Lianhai Zu,^b Yue Jiang,^c Donglu Shi,^{bd} Xiaoming Cai,^e
Yonghong Ni,^{id}*^a Sijie Lin^{id}*^c and Yao Qin^{id}*^b

rsc.li/chemcomm

20 **mp-MXene/TiO_{2-x} nanodots (NDs) structurally composed of micro-porous MXene monolayers embedded with Ti³⁺-doped TiO₂ nanodots were developed for the first time. The drastically enhanced catalytic efficiency (as much as 13 times higher than that of P25) in degrading dye molecules over mp-MXene/TiO_{2-x} NDs is due to a synergistic effect of the pseudo-Fenton reaction and photocatalysis.**

Advanced oxidation processes (AOPs) based on Fenton reactions, which are capable of generating powerful oxidative hydroxyl radicals ([•]OH), have been applied for wastewater treatment for decades. So far, most of the reported Fenton reagents, either traditional Fe²⁺-H₂O₂ homogeneous systems or their recently developed

heterogeneous counterparts,¹⁻⁴ which usually include solid ferrous nanoparticles activating H₂O₂ to trigger a pseudo-Fenton reaction, are iron-based and need a large amount of H₂O₂.⁵ However, the intrinsic chemical instability of iron-based species limits the applications of these reagents under harsh industrial effluent conditions. Moreover, the large H₂O₂ dosage present in iron-based Fenton reagents have been denounced for the cost and environmental issues.⁵ Titanium dioxide (TiO₂) has been well known as a durable and efficient photocatalyst for decades.^{6,7} Recent discovery in several reports^{8,9} has shown that this semiconductor material can accelerate H₂O₂ decomposition by self-doping of low-valence Ti species, making titanium dioxide an emerging generation of titanium-based photo-(pseudo)Fenton bifunctional catalyst, alternative to iron-based heterogeneous Fenton reagents but with better chemical stability and recyclability.

As Zhang *et al.* have reported in eqn (1)–(4):



aided by the ability to cycle between low- and high-valence states, titanium species on the surface of titanium oxide nanoparticles can serve as a lattice shuttle for electron transfer in H₂O₂ activation.⁹ In their work, TiO₂ nanoparticles were first prepared *via* a hydrothermal method and then specially treated in reductive H₂ at high temperature to create TiO_{2-x} with a high density of Ti³⁺ for H₂O₂ activation.

Herein, we synthesized a new composite from Ti₃C₂ MXene,¹⁰⁻¹³ a good source for active low-valence titanium species, denoted as “microporous-MXene-TiO_{2-x} nanodots” (mp-MXene/TiO_{2-x} NDs), which is structurally composed of porous, mono-layered MXene flakes as the skeleton and TiO_{2-x} nanodots embedded evenly on the flake surfaces. The active low-valence titanium species in both the monolayered MXene flakes and the

35 ^{Q3} ^a College of Chemistry and Materials Science, Key Laboratory of Functional Molecular Solids, Ministry of Education, Anhui Laboratory of Molecule-Based Materials, Anhui Key Laboratory of Functional Molecular Solids, Anhui Normal University, 189 Jiuhua Southern Road, Wuhu, 241002, China

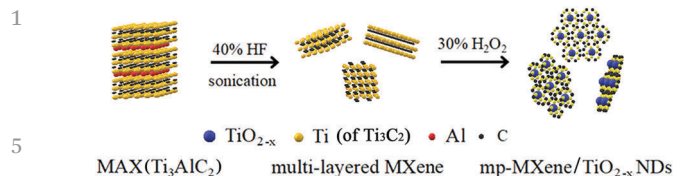
^b The Institute for Translational Nanomedicine, Shanghai East Hospital, The Institute for Biomedical Engineering & Nano Science, Tongji University School of Medicine, Shanghai 200092, China

40 ^c Biomedical Multidisciplinary Innovation Research Institute, Shanghai East Hospital, State Key Laboratory of Pollution Control and Resource Reuse, Shanghai Institute of Pollution Control and Ecological Security, College of Environmental Science and Engineering, Tongji University, 1239 Siping Road, Shanghai 200092, China

^d The Materials Science and Engineering Program, Dept. of Mechanical and Engineering, College of Engineering and Applied Science, University of Cincinnati, Cincinnati, OH, 45221, USA

45 ^e Center for Genetic Epidemiology and Genomics, School of Public Health, Jiangsu Key Laboratory of Preventive and Translational Medicine for Geriatric Diseases, Medical College of Soochow University, Suzhou, China

† Electronic supplementary information (ESI) available: Experimental details; XRD patterns of the pristine MAX, multi-layer MXene and the prepared mp-MXene/TiO_{2-x} NDs; SEM images of the pristine MAX, multi-layer MXene and delaminated mono-layer MXene; TEM images of delaminated mono-layer MXene and the prepared mp-MXene/TiO_{2-x} NDs; XPS depth profiling results; UV-vis absorption of mp-MXene/TiO_{2-x} NDs and multi-layer MXene; specific surface area of mp-MXene/TiO_{2-x} NDs; SEM image of TiO₂-Ti₃C₂; TOC change during the degradation process of RhB; the degradation of RhB on mp-MXene/TiO_{2-x} NDs with and without the attendance of H₂O₂; EPR signal of superoxide radicals ([•]O²⁻) generated in the prepared photo-Fenton catalyst and H₂O₂ system; recyclability assessment of mp-MXene/TiO_{2-x} NDs. See DOI: 10.1039/c8cc05866k



Scheme 1 Schematic illustration of the formation process of mp-MXene/ TiO_{2-x} NDs.

TiO_{2-x} dots as well as the porous structure endow the synthesized mp-MXene/ TiO_{2-x} NDs with high catalytic efficiency in organic pollutant degradation at a low catalyst concentration and low H_2O_2 dosage under both dark and light conditions.

The mp-MXene/ TiO_{2-x} ND catalyst was prepared simply by mixing multilayer MXene (ml-MXene) with 30% H_2O_2 as depicted in detail in ESI 2.1 (ESI[†]) and schematically presented in Scheme 1. The composition and crystalline structure of the as-prepared sample were firstly characterized with X-ray diffraction (XRD) (Fig. S1, ESI[†]). Compared to ml-MXene,^{14,15} the as-synthesized product shows a wider diffraction peak of (002) shifting to a lower angle and no other obvious peaks except a small one at 48° which is assigned to the (200) facets of TiO_2 with an anatase phase (PDF Card No. 21-1272). These results indicate that after treating with H_2O_2 , the ml-MXene is fully delaminated to (quasi-)monolayers meanwhile the titanium species are partially oxidized into TiO_2 , which roughly provides the composition of the synthesized product: monolayered MXene and anatase TiO_2 .

High-resolution X-ray photoelectron spectroscopy (XPS) (Fig. 1a) was performed to determine the detailed chemical states of the Ti element in the obtained composite. The fitting result shows that the peaks at binding energies (BE) of 464.5 and 458.7 eV can be assigned to $\text{Ti}^{4+} 2p_{1/2}$ and $\text{Ti}^{4+} 2p_{3/2}$ in TiO_2 , while the smaller BE peaks at 463.5 and 457.9 eV correspond to electrons of $\text{Ti}^{3+} 2p_{1/2}$ and $\text{Ti}^{3+} 2p_{3/2}$, respectively.^{16–18} This indicates that the obtained TiO_2 might be self-doped with Ti^{3+} . Furthermore, the low-temperature (77 K) electron paramagnetic resonance (LT-EPR) spectrum was measured to elucidate the specific existence state of Ti^{3+} . As shown in Fig. 1b, the weak peak with a calculated g factor of 2.002 can be assigned to superoxide radical anions (O_2^-) from adsorbed O_2 reduced by the surface Ti^{3+} , while the primary peak with a g factor of 1.9588 can be ascribed to Ti^{3+} ions existing in the bulk.¹⁹ These observations provide further evidence that the as-synthesized product is composed of MXene and TiO_{2-x} , contributing to the bulk and surface Ti^{3+} , respectively.

Fig. 2a shows the transmission electron microscopy (TEM) image of the as-synthesized composite product in low-magnification,

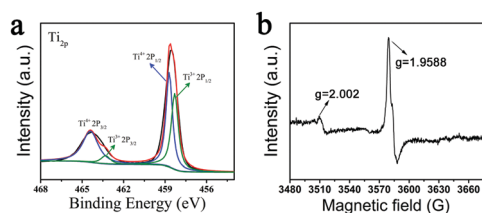


Fig. 1 (a) XPS analysis in the Ti 2p region and (b) low-temperature (77 K) electron paramagnetic resonance (LT-EPR) spectrum of the prepared mp-MXene/ TiO_{2-x} NDs.

presenting the ultrathin, soft, membrane-like feature of the product and confirming the massively fragmented MXene monolayers. As shown in Fig. S2e (ESI[†]), the morphology of the fragmented MXene monolayers is very different from that of the intact ones (Fig. S2c and d, ESI[†]). The pores in Fig. 2a with a size of 10–50 nm may arise from interconnection of these stacked, curled MXene monolayer fragments. Some of these fragmented flakes are observed to stand vertically on the grid, as highlighted with red lines in Fig. 2c, which is a magnified image of the rectangular zone c in Fig. 2b.

The estimated layer thickness of ~ 1 nm further confirms the mono-layered nature of these fragmented MXene flakes.¹⁵ Aside from the vertically standing flakes, typical lattice fringes belonging to the MXene monolayers lying on the grid (Fig. 2c) are identified in Fig. 2d as the (006) plane. Moreover, from Fig. 2c and Fig. S2f (ESI[†]), numerous micropores with sizes smaller than 1 nm can be seen in the MXene flakes. It is reasonable to assume that these micropores arise from the attack of H_2O_2 on the 2D monolayered MXene by “digging” some of the Ti atoms out and oxidizing them *in situ* into TiO_{2-x} dots, leaving the porous skeletons of the MXene flakes. This also explains the vague polycrystalline rings of the selected area electron diffraction (SAED) pattern in the inset of Fig. 2a. The oxidative “etching” process forming “mp-MXene/ TiO_{2-x} NDs” was also verified by the high-resolution XPS depth profiling (XPS-DP) results shown in Fig. S3 (ESI[†]), where compositions at 0 nm, 3 nm, 5 nm and 10 nm beneath the surface of the intermediate product were checked. In the Ti 2p region (Fig. S3a, ESI[†]), from 10 nm to 0 nm beneath the sample surface, where the layers are ready to be delaminated to form the final product, the BE peaks representing the chemical states of $\text{Ti} 2p_{3/2}$ and $\text{Ti} 2p_{1/2}$ electrons in TiO_2 are narrowed and intensified while the peaks at 454.8 eV and 460.2 eV assigned to $\text{Ti} 2p_{3/2}$ and $\text{Ti} 2p_{1/2}$ in Ti_3C_2 respectively become weaker and wider, indicating that the Ti atoms of lower valence near the surface layers of MXene are oxidized gradually into $\text{Ti}(\text{iv})$ in TiO_2 .^{15,16,20} In the C 1s region (Fig. S3b, ESI[†]), approaching the surface layer, the intensified graphitic C–C (sp^2) peak at 284.8 eV indicates that parts of the carbon atoms rearranged into a graphene-like structure by overlapping their sp^2 orbital after the Ti atoms are “dug out” by H_2O_2 oxidation, which is evidenced in Raman characterization (Fig. S4, ESI[†]) as well, thereby leaving a mass of micropores in the parent MXene skeleton flake.¹⁷ The specific surface area of mp-MXene/ TiO_{2-x} NDs was analyzed using a classical BET method and measured to be $\sim 54.56 \text{ m}^2 \text{ g}^{-1}$ (Fig. S5a, ESI[†]). The average pore width calculated using the DFT model was 1.31 nm (inset of Fig. S5a, ESI[†]), corresponding to the size of micropores.

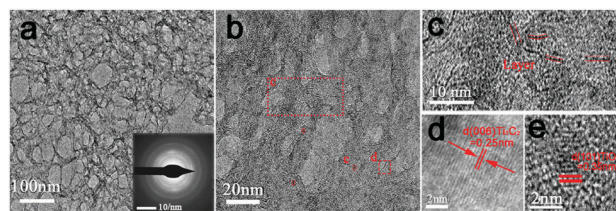


Fig. 2 TEM images (a and b), SAED pattern (inset of a) and high-resolution TEM images (c–e) of mp-MXene/ TiO_{2-x} NDs.

Meanwhile, as shown in Fig. 2b, there are also many black dots (marked with red circles) with a size of ~ 3 nm inlaid in the MXene plane (see Fig. S2f, ESI[†] for additional evidence). The lattice fringes of one of these black dots are presented in the high-resolution TEM image of Fig. 2e, where the d -space is measured to be 0.35 nm, corresponding to the (101) facets of anatase TiO₂. The UV-vis diffuse reflection spectrum was measured to study the optical properties of the synthesized product. As shown in Fig. S5b (ESI[†]), due to the deposited TiO_{2-x} nanodots on the MXene skeleton flakes, the absorption of mp-MXene/TiO_{2-x} NDs behaves as a typical semiconductor with a calculated band gap of 2.2 eV *via* the Kubelka-Munk method, which is quite different from the pristine ml-MXene.

Based on the composition and structural characteristics of mp-MXene/TiO_{2-x} NDs, we evaluated its potential as a heterogeneous photo-Fenton catalyst by degrading several typical model dye molecules. Considering the possible contributions of Ti species in both MXene and TiO_{2-x} dots to a photocatalytic-Fenton reaction, the dosage of the synthesized product and the samples for comparison were determined according to the concentration of the Ti element ([Ti]). For example, a mp-MXene/TiO_{2-x} NDs solution of 150 ppm contains the same [Ti] with a Degussa-P25 (P25) dispersion of 0.25 g L⁻¹. As shown in Fig. 3a, under simulated sunlight irradiation (SSI), rhodamine B (RhB) decomposes very fast with mp-MXene/TiO_{2-x} NDs as the catalyst in the presence of low-dosage H₂O₂: in 10 min, 96% of the RhB molecules (30 mg L⁻¹) were degraded (black square line, [Ti] = 150 ppm, and [H₂O₂] = 0.7 mM) with a TOC removal of 55.4% at 1 h (Fig. S7, ESI[†] TOC analysis). It is noteworthy that even when [Ti] decreases to 30 ppm and 10 ppm, as shown by the red, spherical dotted line and the magenta, downward triangular line respectively in Fig. 3a, the catalytic efficiency is still much higher than that of commercial P25 (navy blue, sideward triangular line).

To investigate the catalytic degradation process, 10 ppm [Ti] was chosen (equivalent to 16.7 mg L⁻¹ P25 or 13.3 mg L⁻¹ TiO₂-Ti₃C₂ (ml-MXene-pure TiO₂ nanoparticles, see ESI 2.2 and Fig. S6, ESI[†])) and the whole process was separately controlled under dark or light irradiation for comparison. In darkness, mp-MXene/TiO_{2-x} NDs, at a concentration as low as [Ti] = 10 ppm and [H₂O₂] = 0.047 mM, showed a considerable degradation effect to

RhB (Fig. 3b, magenta, solid/hollow triangular lines in the first hour) with a TOC removal of 33.6% at 120 min (Fig. S7, ESI[†] TOC analysis). On the other hand, both P25 and TiO₂-Ti₃C₂ had negligible catalytic activity in the presence of the same amount of H₂O₂ without light irradiation (Fig. 3b, navy blue, solid/hollow triangular lines and orange, solid/hollow-dotted lines in the first hour). These observations provide convincing evidence that the pseudo-Fenton catalytic activities in the dark come from the mono-layered Mxene fragments and Ti³⁺ doped TiO₂ nanodots rather than the multi-layered Mxenes and pure TiO₂ nanoparticles. Interestingly, after light was turned on at the beginning of the second hour, as indicated by the magenta, solid triangular line in Fig. 3b, there is a drastic increase in catalytic efficiency over the mp-MXene/TiO_{2-x} ND catalyst, implying that the photocatalytic mechanism could set in synergistically with the pseudo-Fenton reaction, and it greatly accelerates the degradation rate. In contrast, neither P25 (navy blue, solid triangular line) nor TiO₂-Ti₃C₂ (orange, solid dotted line) shows comparative catalytic activity.

The synergetic effect can also be verified *via* the control experiments as shown in Fig. S8 (ESI[†]). When H₂O₂ is removed from the catalysis system (the orange square line), the Fenton reaction becomes blocked, resulting in the decrease of catalytic efficiency. The first-order rate constant over the present photo-(pseudo)Fenton catalysis reaction with mp-MXene/TiO_{2-x} NDs as the catalyst ([Ti] = 150 ppm and [H₂O₂] = 0.7 mM) was calculated to be 19.45 h⁻¹ (14 times the rate constant in the P25-H₂O₂ catalytic system), which is much higher than the reported values of 1.72 and 2.38 h⁻¹ for TiO_{2-x}/H₂O₂ and Fe₃O₄/H₂O₂ systems, respectively.⁹ Besides RhB, the photo-Fenton catalytic performance was tested over the degradation of other dye pollutants as well, such as methyl orange (MO) and methylene blue (MB) at pH = 10.0 and 3.33, respectively (Fig. S9, ESI[†]). The data suggest that the as-prepared photo-Fenton catalyst can work in a wide pH range, which is a significant improvement over traditional Fenton reagents.

The main reactive oxygen species (ROS) were detected through the trapping experiments of radicals using *t*-BuOH, EDTA-2Na and *p*-benzoquinone as the hydroxyl radical (\bullet OH), hole (h⁺) and superoxide radical (\bullet O²⁻) scavenger, respectively.²¹ The experiments were conducted under dark and light conditions separately in order to distinguish the ROS species behind the two different mechanisms. The result under light irradiation is shown in Fig. 4a. The addition of *t*-BuOH (1 mM) has hardly any effect on the degradation efficiency (red dotted line), meaning that \bullet OH radicals are not the functional ROS under light conditions. However, the addition of *p*-benzoquinone (1 mM) distinctly reduced the reaction rate (magenta, downward triangular line), indicating that \bullet O²⁻ radicals are one of the main ROS during the catalysis reaction under light irradiation. This was further confirmed by EPR measurements, as shown in Fig. S10 (ESI[†]), after irradiation with light, the signal for the superoxide radicals becomes stronger along with the stimulation time. Specially, the scavenger of EDTA-2Na (1 mM) greatly weakened the reaction efficiency as shown by the navy blue, upward triangular line. This can be explained from two aspects: first, as a classical hole scavenger, EDTA-2Na removes most of the photo-generated holes which play a main role in oxidizing the dye molecules; second, as a typical chelating agent, EDTA-2Na blocks out the function of active

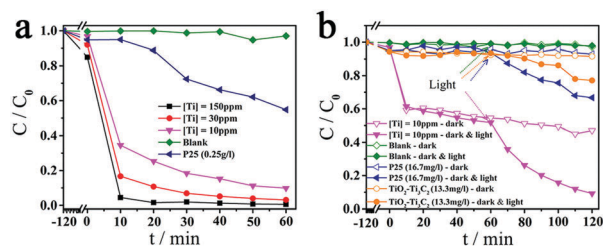


Fig. 3 (a) Degradation of RhB (30 mg L⁻¹) using mp-MXene/TiO_{2-x} NDs at different concentrations of titanium and H₂O₂ with simulated sunlight irradiation (SSI); (b) degradation of RhB (30 mg L⁻¹) upon mp-MXene/TiO_{2-x} NDs and catalysts for comparison under dark (1 h) and light (SSI, 1 h) conditions. For all the above experiments, the pre-dark adsorption-desorption equilibrium process was done for 120 min without adding H₂O₂.

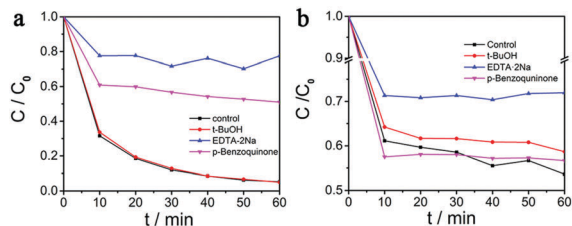
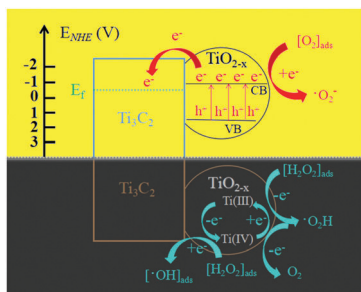


Fig. 4 Degradation of RhB (30 mg L⁻¹) over mp-MXene/TiO_{2-x} NDs ([Ti] = 10 ppm and [H₂O₂] = 0.047 mM) with the attendance of different radical scavengers (1 mM) under (a) light (SSI) and (b) dark conditions.



Scheme 2 Schematic illustration of the degradation mechanisms over the heterostructured mp-MXene/TiO_{2-x} NDs under light (yellow zone) and dark (black zone) conditions, respectively.

Ti³⁺ ions in the catalyst which play a vital role in initiating Fenton reactions. Herein, upon light irradiation, as shown in Fig. 4a, the former is considered to be predominant over the latter.

In contrast, in Fig. 4b, in darkness, the addition of *p*-benzoquinone (1 mM) does not have any inhibitory effect on the reaction rate, while EDTA-2Na (1 mM) shows a considerable inhibitory effect on the catalysis process and *t*-BuOH (1 mM) reduces the catalytic efficiency as well, indicating that •OH radicals instead of •O²⁻ are the main ROS for RhB degradation under dark conditions. Specially, as mentioned previously, the repressing effect of EDTA-2Na under dark conditions is attributed to the strong chelation of Ti³⁺ by EDTA ions. Therefore, a possible mechanism is illustrated in Scheme 2. In the dark, the low-valence titanium species (Ti(III)) near the surface of the TiO₂ dots initiate the pseudo-Fenton reaction, and •OH radicals are generated (eqn (1)) to accelerate the oxidation of organic dye molecules. When light is turned on, the photo-catalysis mechanism starts to set in. Photo-generated electrons (e⁻) combine quickly with the adjacent, dissolved oxygen molecules, which are abundant in the present system due to the continual decomposition of H₂O₂ *via* a pseudo-Fenton process. Consequently, the •O²⁻ radicals are dominantly generated. At the same time, the photo-generated holes (h⁺) are transferred to the hydroxyl terminated Ti₃C₂ skeleton flakes driven by the difference of work function at the heterojunction interface.¹⁶ Therefore, either the pseudo-Fenton reaction in the dark or the photocatalysis-Fenton synergistic mechanism under light benefits from the abundant Ti³⁺ doping and the special Ti₃C₂-TiO_{2-x} hetero-structures. The cyclic performance of the synthesized product is studied, as shown in Fig. S11 (ESI[†]), after 10 cycles, the photocatalytic-Fenton reaction over

the mp-MXene/TiO_{2-x} ND catalyst shows a similar efficiency as the first cycle in the degradation of RhB.

In conclusion, we have developed a novel hetero-structured mp-MXene/TiO_{2-x} ND composite as a photo-Fenton bifunctional catalyst. In addition to holes, •OH and •O²⁻ were detected to be the functional ROS involved under dark and light conditions, respectively. Specially, under light, the high efficiency is accomplished *via* a pseudo-Fenton reaction and photocatalysis mechanism working synergistically together. As a fresh member of the emerging “titanium-based AOP catalyst” family, mp-MXene/TiO_{2-x} ND is promising to find its potential applications in other AOPs, in addition to waste water treatment, owing to its fast response, high efficiency at a very low dosage and a wide working pH range under light and dark conditions.

This work was supported by “2017 and 2018 Fundamental Research Funds for the Central Universities” (Y. Qin), NSFC Grant #21607115 and #21777116 (S. Lin), and NSFC Grant #21571005 (Y. H. Ni).

Conflicts of interest

There are no conflicts to declare.

Notes and references

- X. J. Hou, X. P. Huang, Z. H. Ai, J. C. Zhao and L. Z. Zhang, *J. Hazard. Mater.*, 2016, **310**, 170–178.
- J. G. Shi, Z. H. Ai and L. Z. Zhang, *Water Res.*, 2014, **59**, 145–153.
- Z. Jia, W. C. Zhang, W. M. Wang, D. Habibi and L. C. Zhang, *Appl. Catal., B*, 2016, **192**, 46–56.
- Z. Jia, J. Kang, W. C. Zhang, W. M. Wang, C. Yang, H. Sun, D. Habibi and L. C. Zhang, *Appl. Catal., B*, 2017, **204**, 537–547.
- M. Y. Xing, W. J. Xu, C. C. Dong, Y. C. Bai, J. B. Zeng, Y. Zhou, J. L. Zhang and Y. D. Yin, *Chem*, 2018, **4**, 1359–1372.
- J. Zhang, Q. Xu, Z. Feng, M. Li and C. Li, *Angew. Chem., Int. Ed.*, 2008, **47**, 1766–1769.
- O. A. Osin, T. Y. Yu, X. M. Cai, Y. Jiang, G. T. Peng, X. M. Cheng, R. B. Li, Y. Qin and S. J. Lin, *Front. Chem.*, 2018, **6**, 192.
- Z. H. Liu, T. Wang, X. Yu, Z. X. Geng, Y. H. Sang and H. Liu, *Mater. Chem. Front.*, 2017, **1**(10), 1989–1994.
- A. Y. Zhang, T. Lin, Y. Y. He and Y. X. Mou, *J. Hazard. Mater.*, 2016, **311**, 81–90.
- L. Wang, W. Q. Tao, L. Y. Yuan, Z. R. Liu, Q. Huang, Z. F. Chai, J. K. Gibson and W. Q. Shi, *Chem. Commun.*, 2017, **53**, 12084–12087.
- M. Q. Zhao, X. Q. Xie, C. E. Ren, T. Makaryan, B. Anasori, G. X. Wang and Y. Gogotsi, *Adv. Mater.*, 2017, **29**, 2410–2417.
- C.-F. Fu, X. X. Li, Q. Q. Luo and J. L. Yang, *J. Mater. Chem. A*, 2017, **5**, 24972–24980.
- Y. L. Sun, D. Jin, Y. Sun, X. Meng, Y. Gao, Y. H. Dall’Agnese, G. Chen and X.-F. Wang, *J. Mater. Chem. A*, 2018, **6**, 9124–9131.
- F. Wang, C. Yang, M. Duan, Y. Tang and J. Zhu, *Biosens. Bioelectron.*, 2015, **74**, 1022–1028.
- A. Lipatov, M. Alhabeb, M. R. Lukatskaya, A. Bosen, Y. Gogotsi and A. Sinitskii, *Adv. Electron. Mater.*, 2016, **2**, 2551–2559.
- C. Peng, H. Wang, H. Yu and F. Peng, *Mater. Res. Bull.*, 2017, **89**, 16–25.
- X. Hou, X. Huang, F. Jia, Z. Ai, J. Zhao and L. Zhang, *Environ. Sci. Technol.*, 2017, **51**, 5118–5126.
- T.-S. Yang, M.-C. Yang, C.-B. Shiu, W.-K. Chang and M.-S. Wong, *Appl. Surf. Sci.*, 2006, **252**, 3729–3736.
- F. Zuo, L. Wang, T. Wu, Z. Y. Zhang, D. Borchardt and P. Y. Feng, *J. Am. Chem. Soc.*, 2010, **132**, 11856–11857.
- M. Naguib, M. Kurtoglu, V. Presser, J. Lu, J. Niu, M. Heon, L. Hultman, Y. Gogotsi and M. W. Barsoum, *Adv. Mater.*, 2011, **23**, 4248–4253.
- X. Bai, L. Wang, Y. Wang, W. Yao and Y. Zhu, *Appl. Catal., B*, 2014, **152–153**, 262–270.